Diffusion Dominant Solute Transport Modelling in Fractured Media Under Deep Geological Environment – 12211

S. Kwong* and A.P. Jivkov**

* National Nuclear Laboratory, UK.
** Research Centre for Radwaste and Decommissioning and Modelling and Simulation Centre, University of Manchester, UK.

ABSTRACT

Deep geologic disposal of high activity and long-lived radioactive waste is gaining increasing support in many countries, where suitable low permeability geological formation in combination with engineered barriers are used to provide long term waste contaminant and minimise the impacts to the environment and risk to the biosphere.

This modelling study examines the solute transport in fractured media under low flow velocities that are relevant to a deep geological environment. In particular, reactive solute transport through fractured media is studied using a 2-D model, that considers advection and diffusion, to explore the coupled effects of kinetic and equilibrium chemical processes. The effects of water velocity in the fracture, matrix porosity and diffusion on solute transport are investigated and discussed. Some illustrative modelled results are presented to demonstrate the use of the model to examine the effects of media degradation on solute transport, under the influences of hydrogeological (diffusion dominant) and microbially mediated chemical processes.

The challenges facing the prediction of long term degradation such as cracks evolution, interaction and coalescence are highlighted. The potential of a novel microstructure informed modelling approach to account for these effects is discussed, particularly with respect to investigating multiple phenomena impact on material performance.

INTRODUCTION

Deep geologic disposal of high activity and long-lived radioactive waste is increasingly becoming the preferred option in many countries, where suitable low permeability formation in saturated zone can be found to provide effective long term waste contaminant with minimum impact to the environment and risk to the biosphere. The use of a multi-barrier system, consisting of engineered barriers and a natural barrier by geological formations, could further enhance the containment performance of the repository. By making use of the defence-in-depth principle this helps to maximise the ability to contain the waste and isolate the facility from external influences such as due to groundwater ingress, seismic events etc. A typical deep repository is likely to be hundreds of metres below ground, with the waste sealed in durable containers that are surrounded by low-permeability rock (or clay) barrier to prevent radioactive material leakage into the environment. In the UK, ongoing studies are carried out to assess the merits of different repository concepts, while a programme has been initiated to identify a suitable geological site for the management of high- and intermediate-level radioactive wastes.

One of the main requirements for a suitable deep repository site is that the geological formation surrounding the repository would ensure slow groundwater transport from the repository to the surface. In addition, conditions that would favour geochemical and mineralogical processes to prevent and delay radionuclide transport of dissolved species are also desirable. Further complications may arise as the chemically reactive processes that occur in disposal facilities may be mediated by microbial processes that metabolise the variety of chemical compounds present in transuranic and intermediate level wastes (TRU/ILW), together with organic carbon and hydrogen present in the geological and engineered systems. When groundwater flow is very slow, radionuclide transport dominated by diffusion and sorption, with the additional effects due to the diffusive

transport of reactive species that also leads to chemical zonation around waste packages which could provide additional containment of radionuclides.

As the deep repository system is subjected to a variety of thermo-hydro-chemo-mechanical (THCM) effects over the long 'operational' lifespan, the integrity of the barrier system will decrease over time (e.g. fracturing, corrosion, mineral dissolution etc). It is important that these effects are taken into account when assessing the long-term performance of the repository. Numerical models of groundwater flow, solute transport and chemical processes offer a viable and cost effective means to study the long term evolution of site condition, and aid understanding of the behaviour and mobility of the contaminants.

The work presented here demonstrates the use of the GRM code [1] to modelling the effects of media degradation under the influences of hydrogeological (diffusion dominant) and microbially mediated chemical effects in geological systems with low groundwater flows for deep geological disposal systems.

In addition, ongoing work on microstructure-informed modelling approaches is presented. This aims to bridge the gap between the length scale dictated by the defects in typical repository materials and the continuum scale, thus providing mechanistic understanding of macroscopic parameters, such as permeability and diffusivity, and their evolution. For the purpose of discussion, permeability is used to illustrate the modelling concepts in this paper.

OVERVIEW OF THE GRM CODE

The GRM (Generalised Repository Model) is a computer code [1], originally developed by the Research and Technology department of BNFL (now the National Nuclear Laboratory), to model the long term chemical evolution of both the near surface and deep disposal facilities. GRM is a biogeochemical reactive-transport model that considers kinetic controlled corrosion[1] and microbiological reactions together with equilibrium chemical speciation and mineral reaction. GRM includes a comprehensive set of microbial mediated aerobic and anaerobic kinetic controlled processes that utilise commonly occurring substrates and electron donors and acceptors. GRM models a number of microbial processes, represented by a Michaelis–Menton kinetic formulation [2], including aerobic metabolism; denitrification; fermentation; iron reduction; sulphate reduction; acetogenesis and methanogenesis.

The extent of these microbial processes is determined by input kinetic constants and the concentration of the metabolic substrates. The current microbial data set has been compiled for studies of low level waste [3]. Both organic carbon and hydrogen (H_2) can be utilised as electron donors for the above processes. The corrosion module can consider processes of aerobic and anaerobic corrosion. The later anaerobic process is of prime relevance to geological disposal, where it contributes H_2 electron donor for the above microbial processes. Iron corrosion products also have the potential to control redox potential. Based on the extent of the microbial processes the GRM selects and calculates redox potential (Eh) for a number of redox couples [3] including: oxygen, O_2 / H_2O; nitrate NO_3^- / N_2; iron Fe(III)/Fe(II); sulphur SO_4^{2-} / HS; methane CO_2 / CH_4 and fermentation CH_2O / $CH_3COOH + H_2$.

Using the determined Eh calculated by the kinetic module, the chemical module performs an equilibrium speciation calculation that considers the dissolution and precipitation reactions of minerals and radionuclides and determines pH by charge balance.

The GRM computer code utilises a two-dimensional finite difference approach to consider transport in saturated groundwater. The GRM model also allows species transport from the unsaturated zone to the saturated zone via a release coefficient model, although this is less relevant for deep geological disposal applications.

[1] The primary degradation processes considered in the GRM include cellulose hydrolysis and steel corrosion, although cellulose hydrolysis and the associated gas generation often relates to near surface repository rather than deep geological disposals.

GRM uses a finite difference approach, evolving the system through a sequence of time steps. Due to the wide variety of processes modelled and different time scales involved, GRM uses three main modules to handle the microbial, transport and chemical aspects in sequence.

Reference [1] gives more details of the full suite of microbiological processes, chemical speciation, mineral reaction, including radionuclide solubility and sorption. Reference [4] documents details of a wide range of test cases which have been designed to test the extensive capabilities of the GRM program.

ILLUSTRATIVE MODEL OF A GEOLOGICAL WASTE DISPOSAL PACKAGE

An illustrative two-dimensional reactive transport model has been previously developed [5] to examine the coupled effects of a geological waste disposal package between;

- diffusive and advective transport;
- kinetic controlled microbial processes; and
- equilibrium chemical speciation, mineral and radionuclide dissolution and precipitation.

The present study investigates further the effect of medium degradation on solute transport for such a waste package. The model can be considered to represent a generic case relevant to geological disposal of TRU/ILW where a disposal waste package containing contaminants (uranium) and other multivalent reactive species (iron, sulphate, nitrate) are enclosed in a highly impermeable but reactive medium and where diffusion is the main transport mechanism. Iron is in the form of Fe(II) and represents corrosion products present in waste and containers used. The effect of a sealed waste package container (to physically isolate the waste) is not considered in this scenario. The present model therefore examines the effects that may develop after any such containment is breached. The model examines how the evolving chemical conditions of the repository and diffusive properties of the waste and enclosing medium may affect the containment/mobility of the uranium, when the effect of medium degradation is also considered. The enclosing medium has neutral pH and may represent a low permeability enclosing medium, such as clay or backfill. Along a boundary of the model is an advective transport pathway, which can be considered to represent features such as fractures present in the containment medium. Groundwater that saturates the waste package contains organic matter, and it is assumed that the containment medium of the disposal facility and other engineering maintain reducing conditions external to the waste package. These strongly reducing conditions are represented by the partial pressure of hydrogen (0.99 atm H_2) in the model.

The model is configured in a 2-dimensional array of 20 x 20 cells (Fig. 1) where a single row of 20 cells represents an advective region and 19 adjacent rows of 20 cells represent the diffusive zone (no advective flow) including an area of waste source with kinetic release over time. The model considers an area of 5m by 0.48m. The advective row has a width of 0.1m while the remaining 19 rows representing the diffusive regions are of 0.02m width.

The main diffusive region of interest is within the 19 rows over a width of 0.38m (38cm), including the waste region and enclosing medium. Note that the width (or breadth) of the diffusive region is exaggerated in the figures. A groundwater flow rates of 10 ml/day was considered in the advective region. In the diffusive region of the waste and enclosing medium an effective diffusion coefficient of 1.0E-11 m^2/s and a porosity of 0.15 were considered. Other modelling studies of diffusion in the low permeability clay have considered similar diffusion coefficient values [6].

The waste region (shaded red/purple in Fig. 1) contains uranium at a concentration of 1.0E-03 mol/l of pore fluid. The presence of Fe(II) corrosion products in the form of $FeCO_3$ are considered in the waste. The model also considers that reactive chemical species nitrate and sulphate are present in the TRU/ILW waste in the two regions: region 1 (shaded purple) has concentration of 5.0E-3 mol/l NO_3^- while region 2 (shaded red) has a lower concentration of 1.0E-3 mol/l. The sulphate concentration in both regions is 1.0E-3 mol/l. Chloride is also present in the waste at a concentration of 1.1E-1 mol/l in region 1 or 1.5E-1 mol/l in region 2 (to balance

the nitrate) to provide charge balance to compensate for the additional nitrate in region 1. Chloride is not reactive in the model.

The enclosing diffusive medium (clay) is represented by the calcium and iron containing carbonates (calcite, siderite), which is defined by a partial pressure of carbon dioxide (1.45E-2 atm CO_2) that buffers pH to near neutral conditions. Sulphate minerals present in the clay (gypsum, celesite) similarly control the sulphate concentration in groundwater that saturates the clay. The groundwater that saturates the waste and enclosing clay also contains dissolved organic matter, which in the GRM is represented by an acetate concentration of 9.2E-5 mol/l.

The GRM model was run to simulate a period of 100 years of reaction and diffusion.

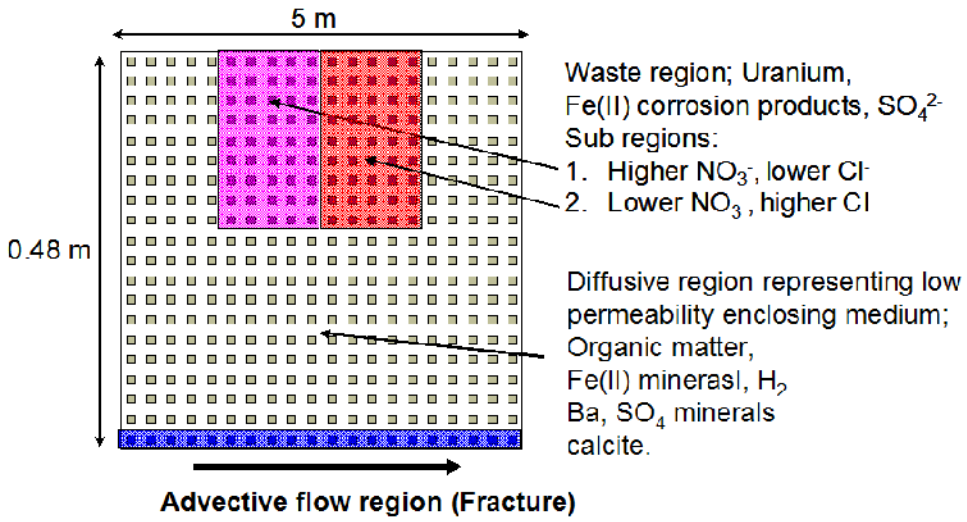

Fig. 1. Schematic illustration of the GRM reactive transport (advection and diffusion) application model [5].

RESULTS AND DISCUSSIONS

The GRM code is used to model an illustrative geological waste disposal package to examine the combined effect of kinetic biogeochemical processes and diffusive dominant transport, under the influence of media degradation and fracture.

Baseline Case

With the initial conditions described above, the system representing a TRU/ILW waste package was modelled for a period of 100 years. Fig. 2 presents summary outputs at the end of the simulation period [5]. Fig. 2a illustrates the diffusive behaviour of chloride, which is both non reactive and non-sorbing. Chloride presents in the waste region (purple region in the figure) diffuses away from the source, such that after 100 years the peak concentration reduces to 4e-2 mol/l (i.e. about 0.88 of the initial maximum concentration in the waste region). The remaining figures illustrate the biogeochemical reactions occurring mediated by microbial processes. The presence of nitrate in the waste results in its rapid reaction by denitrifying bacteria, which utilise organic carbon, H_2 and Fe(II) as electron donors. The oxidation of Fe(II) corrosion products results in the formation of $Fe(OH)_3$ (Fig. 2b), with the amount of $Fe(OH)_3$ formed proportional to the nitrate content of the waste.

The redox potential (Eh) determined by the kinetic routine is illustrated in Fig. 2c, which shows that the oxidation of Fe(II) to Fe(III) in the waste to maintain a higher Eh at around -0.1 volts. It is observed that this

oxidised zone extends into the adjacent clay by diffusion of species and the precipitation of $Fe(OH)_3$, (Fig. 2b). In the majority of the clay zone sulphate reduction occurs due to the dissolved organic matter input from groundwater passing through the advective region that diffuses through the clay zone. Hydrogen present also acts as an electron donor for sulphate reduction. More strongly reducing conditions are established at the inlet of the advective fracture, where sulphate becomes totally reduced by the inflowing organic carbon. The microbial biomass that results from these main reactions of the electron acceptors and donors present is illustrated in Fig. 2d. Most microbial activity is seen to occur in the waste region and at the interface with the clay zone. A further region of microbial activity occurs near the inlet of the advective region.

The resulting diffusive and chemical effect on uranium is illustrated in Fig. 2e and Fig. 2f. In the waste region uranium is in the U(VI) oxidation state and has high solubility. Aqueous uranium becomes mobile and readily diffuses from the waste. Under the sulphate reducing conditions established in the clay, uranium precipitates as UO_2(am) and thus the concentration of dissolved uranium falls significantly compared to that of the non-reactive chloride species (Fig. 2a). The migration of uranium from the waste region is affected to a small extent by the different nitrate contents of the waste in region 1 and region 2 (Fig. 1). Uranium is also precipitated in the advective zone, where the very strongly reducing conditions are developed. The uranium concentration exiting the advective zone is 1.63e-6 mol/l and is a factor of 0.03 lower than that of the maximum concentration in the waste region. As a result of the chemical processes occurring, the concentration gradient of uranium across the diffusion zone is about 30 times that of the non-reactive chloride species.

The effects of media degradation (e.g. fracture and media porosity changes) on solute transport relevant to the long term prediction of containment performance are illustrated below. This highlights the need for a mechanistic understanding and quantification of the macroscopic parameters and their evolution. The later section "Microstructure-Informed Modelling" outlines an ongoing work on microstructure-informed modelling approaches and concepts, and highlights its potential in supporting solute transport modelling that taking account the effects of media degradation.

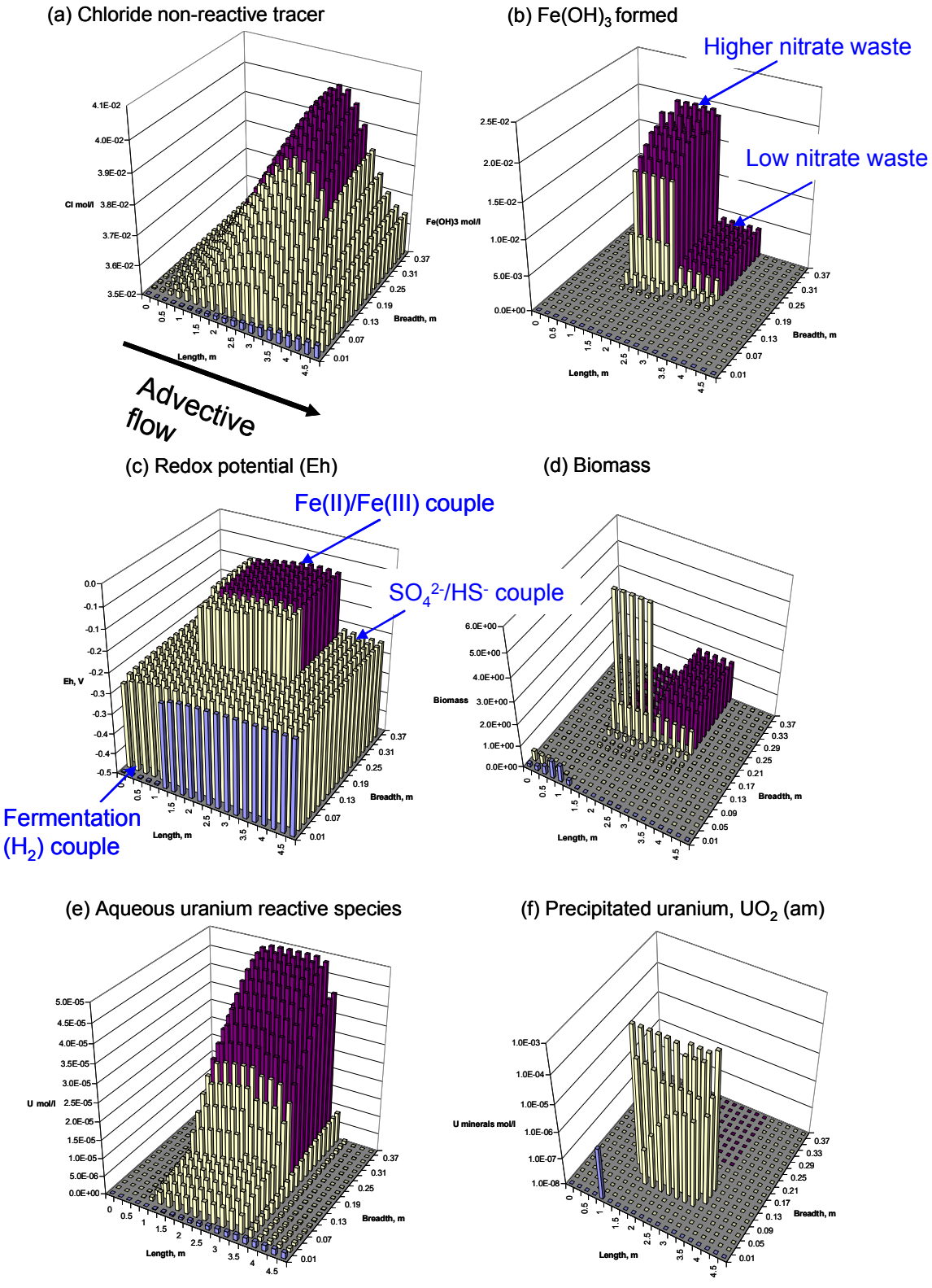

Fig. 2. Baseline Case modelled results of an illustrative waste package in a geological repository after 100 years [5].

Effect of water velocity in the fracture

The effect of fracture on solute transport is investigated by varying the advective flow in the fracture. This may represent a situation over time where the advective flow increases in response to the development of cracking, or a decrease in flow resulted from clogging of pore spaces due to precipitation actions. The non-reactive and non-sorbing chloride clearly illustrates the potential influence of advective flow in the fracture. With low water flow rate in the fracture, the peak chloride concentration in the waste region remains high and only reduces slightly to 4.8e-2 mol/l (Fig. 3a). This relates to the reduced 'flushing' effect of the lower flow (velocity) in the fracture, and leads to a lower concentration gradient (between the waste source and fracture regions) and a reduced diffusive flux away from source. The effect of the higher flow in the fracture is evident in Fig. 3b, showing chloride concentration at significantly reduced levels.

Most of the biomass (resulting from microbial activity) occurs in the waste region and is similar to the Baseline case. The effect on biomass production is most significant near the inlet region where a strongly reducing condition is established with increasing flow rate, (Fig. 3d). Fig. 3e and Fig. 3f show the computed aqueous uranium for the low and high fracture flow rates respectively. While there is little effect on the mobile species near the waste region, significant difference in aqueous uranium concentrations occur along the fracture at a small distance from the inlet. This is closely related to the 'flushing' effect due to the flow in fracture. Some effect on the aqueous uranium concentrations is apparent in a region adjacent to the fracture due to changes in concentration gradient, in addition to the effect of uranium precipitation (Fig. 3g and Fig. 3h). For the case with higher advective flow the modelled result shows that uranium precipitates further downstream in the fracture.

Effect of media porosity

The effect of porosity changes within the waste region is illustrated by varying the porosity and the effective diffusion coefficient[2] (D_E)) of the media. Over the long time scale typical of geological disposal applications, the porosity of the enclosing media may change over time as the pore spaces evolve under the influence of various effects such as degradation due to chemical effects, corrosion or high level irradiation. Modelled results are presented below for two situations: one with reduced porosity θ= 0.1 and D_E= 5.8E-12 m^2/s; the other with an increased porosity θ= 0.2 and D_E= 1.5E-11 m^2/s. (this compares with θ= 0.15 and D_E= 1.0E-11 m^2/s for the Baseline Case).

The non-reactive chloride migrates away from the source region under the diffusive action only, where the peak concentration decreases with increasing porosity due to the higher diffusive flux away from the source, (Fig. 4a and Fig. 4b). Similar to the Baseline case, most of the biomass occurs in the waste region and adjacent area (Fig. 4c and Fig. 4d), with an increase in porosity leading to a slight increase in biomass production in these areas. The biomass area adjacent to the waste is also seen to spread over a slightly wider area for higher porosity due to the enhanced diffusion rate. Biomass is also seen to occur near the fracture inlet region where a strongly reducing condition is established. The effect of porosity change is negligible in this region as this is dominated by the advective flow.

Fig. 4e to Fig. 4h show the effect of porosity change on uranium under the combined influence of diffusive and chemical actions. It is interesting to note that the higher porosity case gives a higher peak aqueous uranium concentration, Fig. 4f. This behaviour is in contrary to the situation for the non-reactive chloride, but can be explained by the increasing chemical effect seen in the higher porosity case with increasing uranium precipitation (Fig. 4h). This illustrates the complexity of solute transport behaviour that could occur in a waste disposal facility, due to the interplay between kinetic biogeochemical processes, advection and diffusion.

[2] In saturated conditions, the effective diffusion coefficient (D_E) of a solute in a porous medium can be estimated from the solute's diffusion coefficient in water (D_o) using the so-called MQ model [7]: $D_E = D_o\theta^{\frac{4}{3}}$,where θ is the porosity of the medium.

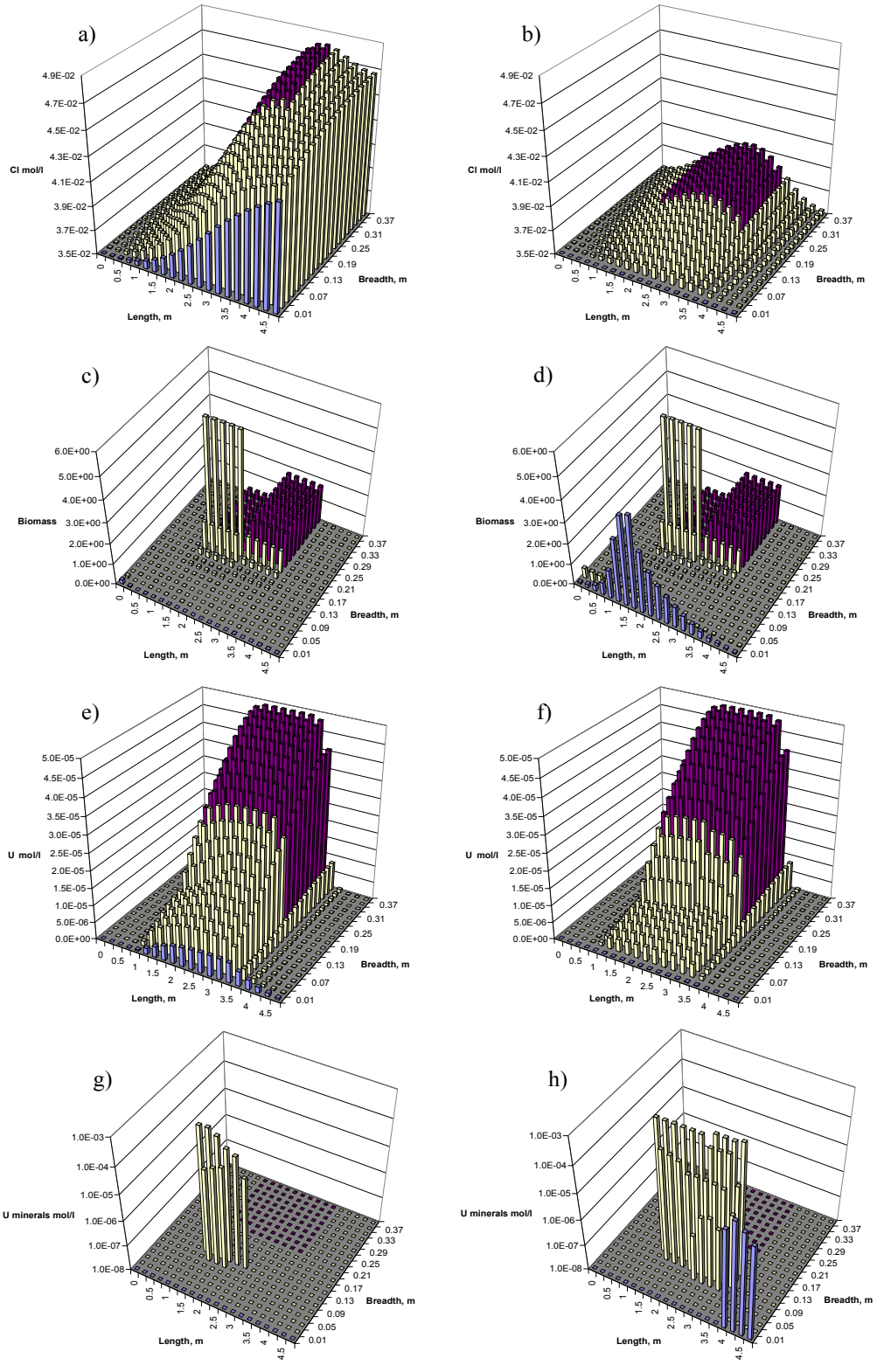

Fig. 3. Modelled results after 100 years showing the effect of advective flow in fracture, with a factor of 0.1 lower (left) and a factor of 10 higher (right).

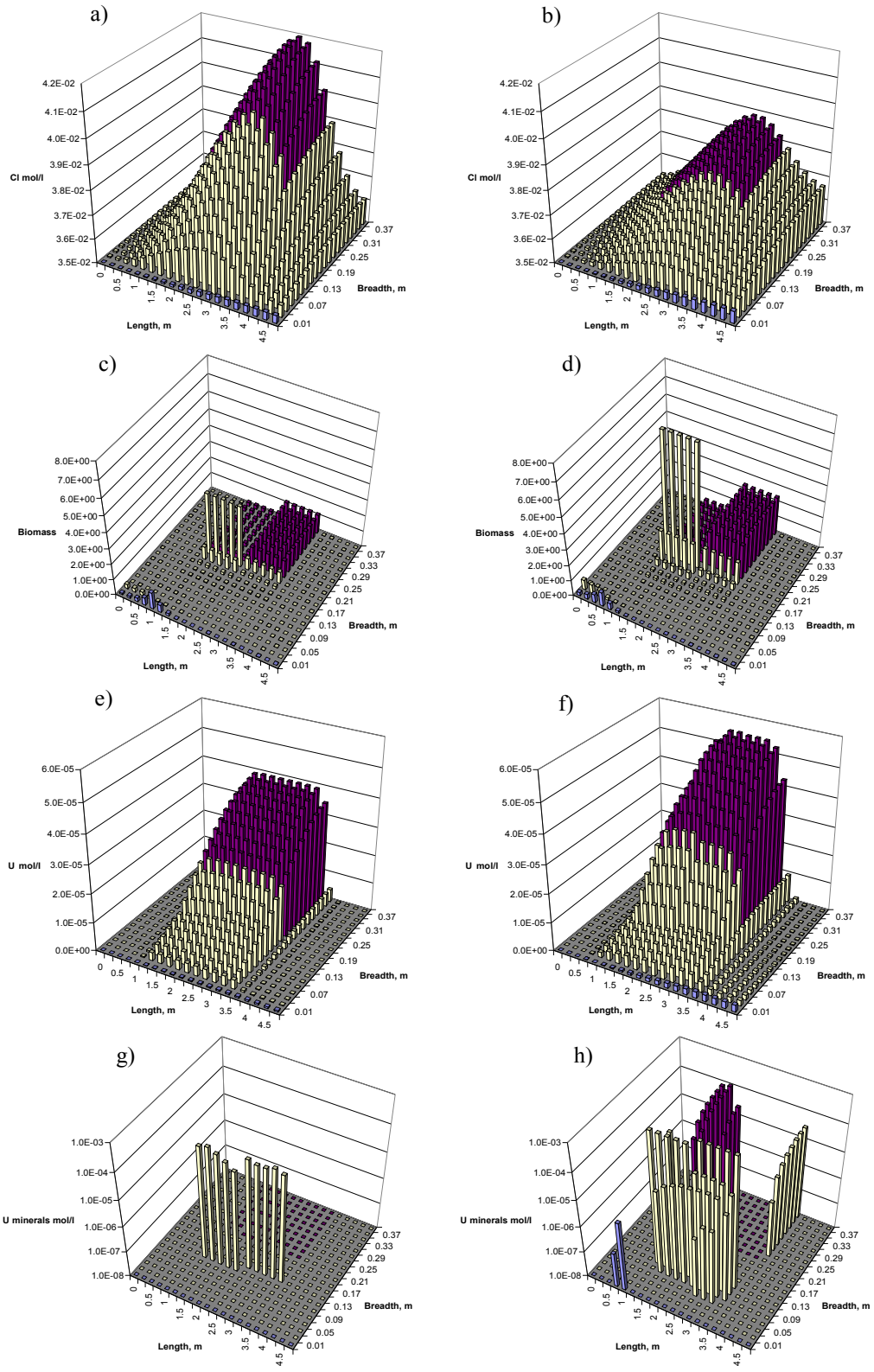

Fig. 4. Modelled results after 100 years showing the effect of porosity change in media, with porosity decrease to 0.1 (left) and porosity increase to 0.2 (right).

MICROSTRUCTURE-INFORMED MODELLING

Most of the barriers in the repository, apart from the metallic canisters, can be considered as porous quasi-brittle media. Their ability to contain radioactive species depends largely on their low permeability, due to poor connectivity of the pore spaces. The pore space, however, may evolve with time over an extended period due to various mechanisms, such as mechanical or chemical damage, electrochemical or bacterial corrosion and high level irradiation. All of these will cause the integrity of the barrier system to decrease over time, or generally referred here as degradation. The pore space changes will yield an evolution in permeability. Predicting this evolution is of key importance for the performance assessment of the engineered barriers system over long time scales, such as for supporting the continuum modelling described above. For solute transport model predictions, one may need to consider the two main characteristics of the media, namely the pore space and the quasi-brittleness.

The physical pore space of containment media generally consists of a complex system of pores, some of which connected by “throats”. The system can be considered as a discrete network of pores and throats at a sufficiently large length scale, conveniently called meso-scale. This length scale is dictated by the distances between the pores, or equivalently by the lengths of the throats. At the meso-scale the fluid flow can be considered a continuum process. The hydraulic permeability emerges as a macroscopic/engineering property of the medium from a fluid flow mediated by the pore space structure. This view can be conveniently captured by the so-called pore-network models (PNM) [8]. A PNM contains a set of pores (e.g. spheres of different radii) and connected by throats (e.g. cylinders with different radii) such that the pores residing at the sites of a regular lattice and throats are linked with some neighbouring pores. Constructing a sufficiently realistic, microstructure-informed, PNM have the potential to allow for fast calculation of fluid flow and macroscopic permeability. The pore space changes, and the resulting evolution of permeability, can then be studied using a collection of meso-scale models, each of which represents a particular pore space changing mechanism. These models will interact with the PNM to exchange information about pore space changes and possibly between themselves when the development of one process affects the development of another.

Processes operating within the pore space, e.g. chemical, electrochemical or bacterial, can be represented by a number of PNMs. Each of these models solves their own boundary value problems and evolves the pore space according to their own time scales. This offers a possible way to study the effect of multiple physical phenomena (at multiple time scales) on the macroscopic permeability. The approach is applicable to situations where the pore space is changed continuously by the degrading mechanisms. The situation is more complex when the damage to the solid phase is discrete, as in the case of micro-cracking when the major micro-cracking induced driving force is a discrete event such as external mechanical loading.due to seismic events or ground motions.

The quasi-brittleness is an important characteristic to be considered with respect to modelling micro-cracking. It derives from the understanding that the medium is elastic-brittle at the meso-scale, but the creation and accumulation of spatially distributed micro-cracks (damage) with loading produces a non-linear emergent/macroscopic deformation response. The damage evolution is thus primarily controlled by the creation, competition and coalescence of micro-cracks. Capturing all these processes with continuum fracture mechanics models is not possible. A promising alternative approach is offered by the so-called discrete particle methods [9]. These models represent the solid phase of the medium with a set of sites connected by bonds. This is similar to the manner pore space is represented in a PNM. The model consists of sites residing at the centres of appropriately defined solid-phase grains, and using bonds to represent the relative deformation between the connected (or coordinated) grains. The arrangement of the sites and the deformation behaviour of the bonds play key role in the macroscopic behaviour of the site-bond assembly. Special site arrangement and bond behaviour have been recently developed to allow for the resulting site-bond model (SBM) to represent the macroscopic elastic behaviour of solids [10]. This provides a major prerequisite to support subsequent realistic modelling of damage.

With respect to the solid phase, the pore space can be considered as a system of spatially distributed defects of different sizes. This effectively establishes a spatial relationship (or a "map") between the properties of a PNM, e.g. pore sizes distribution in the model, and the failure properties of the bonds in a corresponding SBM

of the solid-phase. The model therefore implies, within a given space, the larger the pore in the PNM the lower the strength of the corresponding bond in the SBM. The damage evolution in a SBM can be represented "naturally" as bonds fail when their failure strengths are reached during mechanical loading. This approach has been applied for predicting the macroscopic stress-strain behaviour of cement under tensile and compressive loading using microstructure data only [11]. The model was able to reproduce experimentally measured behaviours, including quasi-hardening and complex softening branches. This suggests that the SBM could provide reasonable damage evolution predictions that can be used to inform pore space changes in the PNM. The link between the two models is an ongoing work and is not reported here. The focus here is on the realistic representation of the pore space. A simplified pore space changing mechanism, mimicking damage, is used to illustrate how this will be used for predicting permeability evolution.

Early PNMs were based on a cubic lattice with a maximum pore coordination of six [12]. Later experimental studies showed that pores with larger pore coordination numbers (PCN) can be substantial fractions of all coordinated pores [13]. These have led to the proposal of PNMs with larger maximum PCN, e.g. 26 in [14], based on cubic support. Although such PNMs are topologically admissible, they are physically unrealistic because a large numbers of throats intersect at points that are not pores. Furthermore, for a given average PCN the existing models reproduce only one PCN spectrum, i.e. number fractions of pores coordinated by different numbers of throats. This spectrum may not correspond to experimentally determined spectra, such as in [13]. A novel lattice support for PNM construction has been recently proposed and justified [15, 16]. This supports an assembly of truncated octahedrons that fills the space compactly, as shown in Fig. 5a. The unit cell of the assembly that illustrates the pore position and the possible coordinating throats are shown in Fig. 5b. Firstly, the support allows for covering pore coordination numbers up to 14, which is sufficient for all practical purposes, without compromising the physical realism of the resulting network. Secondly, the presence of two types of possible throats, T_1 along the principal directions of the cell and T_2 along the body diagonals, makes the model very flexible for representing different coordination spectra in a pore space with a given average coordination, Z. This feature is explored in detail in [15], and is not presented here.

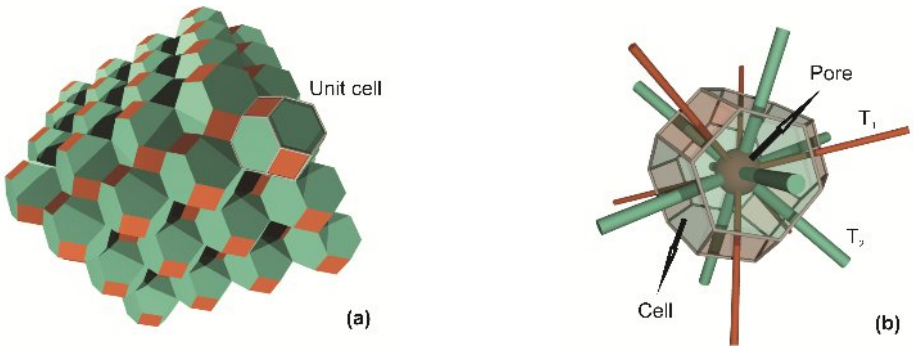

Fig. 5. Lattice support for pore network construction (a) and unit cell (b) showing a pore with all possible throats.

The PNM construction from this support starts with the distribution of pore sizes within cells according to an experimental pore size distribution. These are then linked by all possible throats with sizes distributed according to an experimental throat size distribution. Only a fraction of all throats are made conductive using an elimination process with two different elimination numbers, $0 < E_1 < 1$ and $0 < E_2 < 1$, for the two types of throats, respectively. For each throat a random number $0 < E < 1$ is generated and if $E < E_i$ ($i = 1, 2$) the throat is accepted as conductive. The pores that are coordinated by conductive throats form the initial conducting pore space. The number fractions of pores coordinated by different numbers of conductive throats define the PCN spectrum, which should be matched with experimental data if available. The average PCN of the system, Z, is the minimum experimental requirement for the PNM construction, but as mentioned earlier a given Z can be achieved with a continuum set of (E_1, E_2), each of which producing a different PCN spectrum. The non-conductive throats are left in the system as they represent possible links between pores that can be created by

the evolution of damage. Currently, the conductive throats are assigned local conductivity values proportional to their cross sectional area. This effectively represents a laminar flow in cylindrical pipes [15], and is equivalent to the assumption that all throats in the real pore space having identical local morphologies or shapes. Should experimental data for local morphologies become available, e.g. in terms of conductivity distribution; it could be used to distribute local conductivities in a manner similar to the throat sizes. The length scale of the model thus constructed is calculated from the distributions of pore sizes and conductive throat sizes that are based on experimental porosity data [15].

To illustrate the model performance, pore space data for Ordinary Portland Cement (OPC) obtained with synchrotron micro tomography is used. The data available contain accessible porosity, □□ distribution of pore sizes; distribution of throat sizes and numbers of pores coordinated by different numbers of throats. The cumulative pore and throat size distributions are shown in Fig. 6. These are used to distribute the pore and throat sizes in the model. The size of a pore or a throat is determined from the corresponding cumulative distribution with a generator of uniformly distributed random numbers between zero and one.

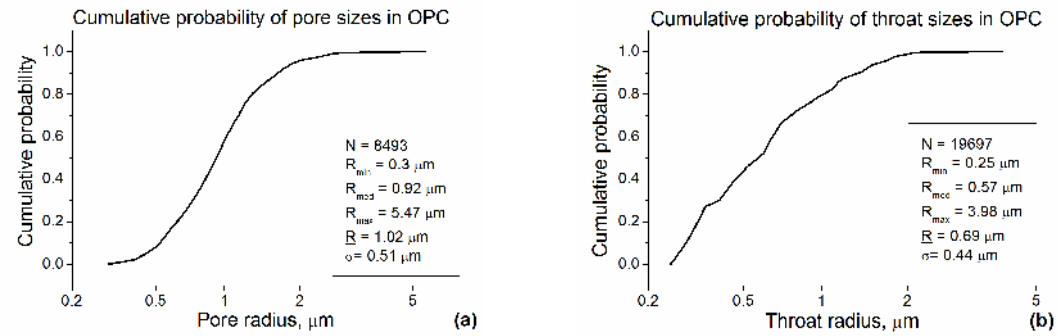

Fig. 6. Cumulative pore radius (a) and throat radius (b) distributions in OPC determined from pore space analysis of 3D microtomography images.

Fig. 7a shows the experimentally determined PCN spectrum as well as the spectrum produced by the model. Of all possible combinations (E_1, E_2) providing the experimentally determined Z (depicted) the combination providing a spectrum closest to the experimental one is selected (depicted). Fig. 7b illustrates a segment of the pore network constructed with the model PCN spectrum and the pore and throat size distributions from Fig. 6. The total porosity and the calculated model length scale are depicted.

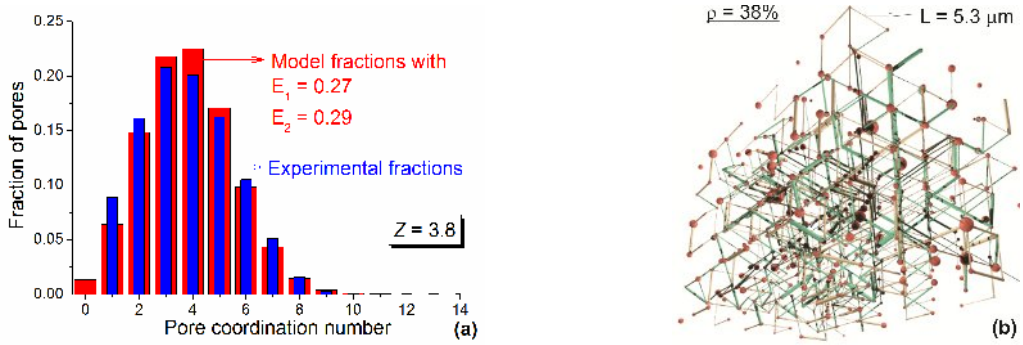

Fig. 7. Experimental and model pore coordination number spectra (a) and an illustration of the resulting pore network used for permeability calculations (b). (Note that the pore and throat radii are not to scale.)

Permeability of the PNM is calculated assuming fully saturated conditions. The model is subjected to experimental boundary conditions and constitutes a boundary value problem. The mathematical description of this problem is described previously [15]. The numerical solution of the problem provides the pressures values in all pores and the fluxes in all throats, with which the macroscopic permeability can be readily calculated. The model is calibrated against an experimentally measured permeability by varying the local conductivity values of the throats, i.e. by varying the coefficient of proportionally between throat conductivity and cross section area. This is given in more detail in [16] for two different sandstones. The model illustrated in Fig. 7b was calibrated against a measured permeability of OPC, $K = 1.1\times10^{-18}$ m^2. The model contains approximately 32,000 pores and 224,000 throats, of which approximately 60,800 were initially conductive and 163,200 were initially non-conductive. The evolution of its permeability with pore space changes was then investigated.

A heuristic argument [15 is employed to mimic mechanical damage without interaction with a corresponding solid-phase model. It is assumed that at a given simulation step the solid phase fails around the pore which is simultaneously the largest and best connected. This pore is not considered in the subsequent simulation steps. The throats coordinating the pore that are currently conductive are then enlarged proportionally by a predefined factor, S, called damage factor. This has the effect of increasing the local conductivities for subsequent simulation steps. The throats coordinating the pore that are currently non-conductive are not enlarged but are made conductive after the step, with conductivities proportional to their cross section area. The two processes represent local pore space enlargement and creation of new flow channels, respectively, resulting from mechanical damage. The local changes contribute to changes in global porosity and permeability, which are re-calculated after each failure event. The main unknown in the procedure is the damage factor, S, i.e. the relation between a mechanical micro-failure and the increase of local pore space geometry and conductivity. Further work on the determination of the damage factor is therefore needed.

Simulations have been performed with two values of the damage factor, S = 1.3 and S = 1.6, following 250 failure events. Fig. 8a shows the evolution of the model porosity with the failure events for the two damage factors. Current porosity is normalised by the initial porosity. The ratio can be considered as a measure of global pore space damage. As expected the results are highly dependent on the choice of S. Fig. 8b shows the predicted evolution of permeability (for the two the damage factors) against the evolution of porosity or global pore space damage. These results may not seem intuitive at first. For a given global damage (or porosity) the system with S = 1.3 has a higher permeability than the system with S = 1.6. Alternatively, the system with S = 1.3 attains a given permeability at a lower global damage than the system with S = 1.6.

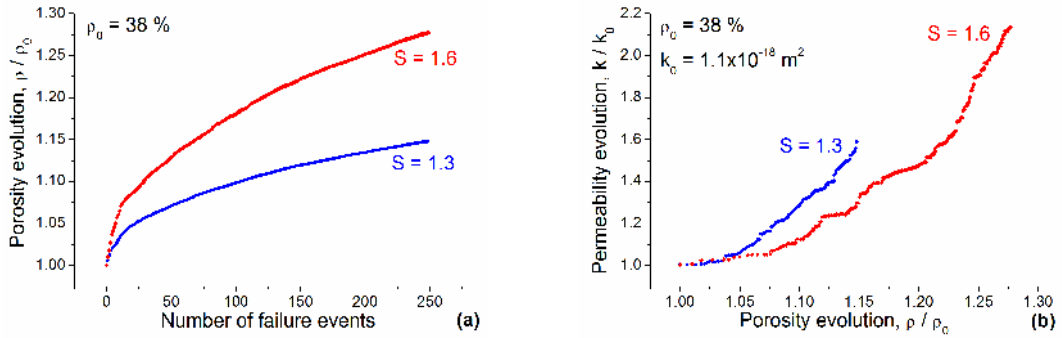

Fig. 8. Predicted evolution of porosity (a) and permeability (b) for OPC using different local damage factors.

The above result implies there may not be a simple relation between the evolutions of permeability and global damage. This outcome seems to be consistent with its non-evolutionary counterpart of the well-known fact that permeability is not linearly related to porosity. The permeability evolution depends, in a complex manner, on the collective outcomes from accumulating micro-failures. This supports strongly the modelling methodology proposed here, because it is unlikely to be able to capture this complexity without using a detailed modelling approach such as the realistic microstructure-informed models. It is worth noting, that the

jumps in the permeability curves represent truthful physical events, where a particular pore space failure leads to the creation of a "shortcut" in the fluid path and hence a stepwise increase in the macroscopic permeability. In practice, the local damage factor, S, can be calibrated against experimental data for the changes in macroscopic permeability in specimens subjected to mechanical damage. Such experiments are planned for the near future and will be used in conjunction with the planned link between the PNM and the corresponding SBM of the solid phase.

Several strengths of the proposed model are worth mentioning. Firstly, the model is applicable to any porous quasi-brittle material provided the required supporting microstructure data is available. Secondly, the model can be used at different length scales, such that the meso-scale referred here can be replaced by a different length scale to reflect a particular system of defects. For example, it can be used as a productive alternative to the discrete fracture network approaches for modelling fractured rock. In this case, the sites of the PNM will be the intersections of rock fractures and the bonds of the PNM will be the segments of these rock fractures between the intersections. The "meso-scale" here will be dictated by the lengths of the fractures. Regarding the ability of the model to describe complex pore and solid phase systems the following additional features can be readily introduced. For the pore space:

- connectivity anisotropy and/or heterogeneity via assignment of different elimination numbers to throats in different directions and/or domains of the model; and
- conductivity anisotropy and/or heterogeneity via assignment of different conductivity values to throats in different directions and/or domains of the model.

For the linked solid phase:

- deformation anisotropy and/or heterogeneity via assignment of different mechanical behaviour to bonds in different directions and/or domains of the model.

And for both systems when linked:

- material texture via assignment of different cell sizes in the principal directions. Several of these features are subjects of ongoing works.

CONCLUSIONS

The GRM code is used to examine the effects of media degradation for a geological waste disposal package, under the combined hydrogeological (diffusion dominant) and chemical effects in low groundwater flow conditions that are typical of deep geological disposal systems.

An illustrative reactive transport modelling application demonstrates the use of the code to examine the interplay of kinetic controlled biogeochemical reactive processes with advective and diffusive transport, under the influence of media degradation. The initial model results are encouraging which show the disposal system to evolve in a physically realistic manner.

In the example presented the reactive-transport coupling develops chemically reducing zones, which limit the transport of uranium. This illustrates the potential significance of media degradation and chemical effect on the transport of radionuclides which would need to be taken into account when examining the long-term behaviour and containment properties of the geological disposal system.

Microstructure-informed modelling and its potential linkage with continuum flow modelling is a subject of ongoing studies. The approach of microstructure-informed modelling is discussed to provide insight and a mechanistic understanding of macroscopic parameters and their evolution. The proposed theoretical and methodological basis for microstructure-informed modelling of porous quasi-brittle media has the potential to develop into an explanatory and predictive tool for deriving mechanism-based, as opposed to phenomenological, evolution laws for macroscopic properties. These concepts in micro-scale modelling are likely to be applicable to the diffusion process, in addition to advective transport illustrated here for porous media.

REFERENCES

1. S. Kwong. (2009a). Program User's Guide for the code GRM, Version 6.1. NNL Report.
2. P. L. McCarty and F. E. Mosey. (1991). Modelling of Anaerobic Digestion Processes (A Discussion of Concepts), Water Sci. Technol. 24 No.8, pp.17-33.
3. J. Small, M. Nykyri, M. Helin, U. Hovi, T. Sarlin and M. Itävaara, M. (2008). "Experimental and modelling investigations of the biogeochemistry of gas production from low and intermediate level radioactive waste". Applied Geochemistry Vol 23, pp.1383-1418.
4. S. Kwong. (2009b). Program Verification Report for the code GRM, Version 6.1. NNL Report.
5. S. Kwong and J.S. Small. (2010) "Coupling Diffusive Transport and Chemical Reaction in the Generalised Repository Model (GRM)", Proceedings of WM2010: The Waste Management Symposium 2010, Phoenix, US.
6. E.C. Gaucher, P. Blanc, J.M. Matray and N. Michau. (2004). "Modeling diffusion of an alkaline plume in a clay barrier". Applied Geochemistry Vol 19, pp.1505-1515.
7. R.J. Millington and J. M. Quirk, "Permeability of porous solids". Trans. Faraday Soc. 57:1200-1207 (1961).
8. M.J. Blunt, M.D. Jackson, M. Piri and P.H. Valvatne, (2002). "Detailed physics, predictive capabilities and macroscopic consequences for pore-network models of multiphase flow". Adv. Water Resour. Vol 25, pp. 1069-1089.
9. P.A. Cundall and R.D. Hurt. (1992). "Numerical modelling of discontinua". Eng. Comput. Vol 9, pp. 101-113.
10. A.P. Jivkov and J.R. Yates, "Regular site-bond models for solids at meso-scale". To appear in J. Mech. Phys. Solids.
11. A.P. Jivkov, M. Gunther and K.P. Travis. (2011). "Site-bond models for porous quasi-brittle media". Proceedings of "Geological Disposal of Radioactive Waste: Underpinning Science and Technology" Conference 2011, Loughborough, UK.
12. P.C. Reeves and M.A. Celia. (1996). "A functional relationship between capillary pressure, saturation and interfacial area as revealed by a pore-scale network model". Water Resour. Res. Vol 32, pp. 2345-2358.
13. A.S. Al-Kharusi and M.J. Blunt. (2007). "Network extraction from sandstone and carbonate pore space images". J. Petrol. Sci. Eng. Vol. 56, pp. 219-231.
14. A. Raoof and S.M. Hassanizadeh. (2010). "A new method for generating pore-network models of porous media". Transp. Porous Media Vol 81, pp. 391-407.
15. A.P. Jivkov and C. Hollis, "A novel site-bond support for pore network construction and application to permeability calculations". To appear in Transp. Porous Media.
16. A.P. Jivkov and J.E. Olele. (2011) "Novel lattice models for porous media". Proceedings of MRS2011 XXXV International Symposium "Scientific Basis for Nuclear Waste Management" 2011, Buenos Aires, Argentina.